Low-Cost Sensorless Control of Brushless dc Motors with Improved Speed Range

Gui-Jia Su and John W. McKeever

Oak Ridge National Laboratory
National Transportation Research Center
2360 Cherahala Blvd.
Knoxville, Tennessee 37932
Email: sugj@ornl.gov

Abstract *** - This paper presents a low-cost position sensorless control scheme for brushless dc motors. Rotor position information is extracted by indirectly sensing the back EMF from only one of the three motor-terminal voltages for a three-phase motor. Depending on the terminal voltage sensing locations, either a low-pass filter or a band-pass filter is used for position information retrieval. This leads to a significant reduction in the component count of the sensing circuit. The cost saving is further increased by coupling the sensing circuit with a single-chip microprocessor or digital signal processor for speed control. In addition, a look-up-table based correction for the non-ideal phase delay introduced by the filter is suggested to ensure accurate position detection even at low speed. This extends the operating speed range and improves motor efficiency. Experimental results are included to verify the proposed scheme.**

I. INTRODUCTION

Because of their higher efficiency and power density, permanent magnet (PM) motors have been widely used in a variety of applications in industrial automation and consumer electric appliances. PM motors can be classified into two major categories with respect to the shapes of their back EMF waveforms, PM AC synchronous (PMAC) motors with sinusoidal back EMF and brushless dc (BLDC) motors with trapezoidal back EMF. A PMAC motor is typically excited by a three-phase sinusoidal current. On the other hand, a BLDC motor is usually powered by a set of currents having a quasi-square waveform. This excitation can be conveniently accomplished with a full-bridge voltage source inverter. An attractive feature of this approach that makes it suitable for a low-cost drive system is the resulting simplicity of current control by means of rotor position sensing.

PM motor drives require a rotor position sensor to properly perform phase commutation and/or current control. For PMAC motors, a constant supply of position information is necessary; thus a position sensor with high resolution, such as a shaft encoder or a resolver, is typically used. For BLDC motors, only the knowledge of six phase-commutation instants per electrical cycle is needed; therefore, low-cost Hall-effect sensors are usually used.

To further reduce cost and improve reliability, such position sensors may be eliminated. Furthermore, sensorless control is the only choice for some applications where those sensors cannot function reliably because of the harsh environments. The BLDC motor provides an attractive candidate for sensorless operation because the nature of its excitation inherently offers a low-cost way to extract rotor position information from motor-terminal voltages. In the excitation of a three-phase BLDC motor, except for the phase-commutation periods, only two of the three phase windings are conducting at a time; and the non-conducting phase carries the back EMF. Exploring this feature, many indirect position detection methods, which sense the back EMF from the non-conducting phase, have been reported in the literature [1-9].

In most of the reported approaches, all three motor-terminal voltages are required. One well-known method is to use filters to extract rotor position information. The position information is then fed to a microprocessor or digital signal processor (DSP) for phase commutation and speed control. Three identical sensing circuits are thus required, resulting in a large part count. As the price of microprocessors and DSPs falls sharply, the cost of the sensing circuit becomes increasingly significant. Another method in [4] is based on the detection of the instants at which the freewheeling diodes of the open-phase leg start conducting. Although it can provide uniform control performance over various operating conditions, this scheme requires complicated sensing circuits and special chopping patterns.

One disadvantage of the trapezoidal back EMF is the requirement for accurate stator current commutation control. The torque developed in a PM motor with a trapezoidal back EMF is very sensitive to the relative phase of the quasi-square wave currents imposed by the inverter with respect to the back EMFs [10]. A small phase error in commutation can produce significant pulsating torques in such drives and generate extra copper losses as a result of a circulating current on the "open" phase that should not conduct. Accurate phase information about the back EMF is thus required to minimize the torque ripple due to phase commutations and to avoid the additional losses. Filter-based methods often suffer from this vulnerability because of the speed-dependant characteristics of the derived position information. They rely on the filters to introduce a fixed phase delay, typically $\pi/6$ or $\pi/2$, which is

* Prepared by Oak Ridge National Laboratory, managed by UT-Battelle, LLC, for the U.S. Dept. of Energy under contract DE-AC05-00OR22725.

impossible over a wide frequency or motor speed range for most filter designs. Therefore, BLDC motors based on such sensorless schemes have a limited speed range, and their performance in terms of maximum torque per ampere capability and efficiency deteriorates as the speed drops.

This paper presents a low-cost sensorless control scheme for BLDC motors. Rotor position information is derived by filtering only one motor-terminal voltage. This leads to a significant reduction in the component count of the sensing circuit. The cost saving is further increased by coupling the sensing circuit with a single-chip microprocessor or DSP for speed control. In addition, a look-up-table based correction for the non-ideal phase-delay introduced by the filter is suggested to ensure accurate position detection even at low speed. This extends the operating speed range and improves motor efficiency.

II. Review of Filter-Based Sensorless Control of Brushless dc Motors

A. Brushless dc Motor

Fig. 1 shows the excitation of a three-phase BLDC motor that consists of a PM motor characterized by a trapezoidal back EMF and a voltage source inverter. The PM motor is represented by an equivalent circuit consisting of a stator resistance, inductance, and back EMF connected in series for each of the three phases with the mechanical moving portion omitted. The figure also shows the desired stator excitation currents, i_a, i_b, and i_c, that the inverter should provide and their relationship with the back EMFs, e_a, e_b and e_c. The currents in each phase should have a rectangular waveshape and must be in phase with the back EMFs of the corresponding phase so that the flat top of the trapezoidal back EMF waveform is well matched to the quasi-square wave current waveform. Such currents will develop a constant power and thus a constant torque delivered to the rotor.

In the BLDC mode, only two of the three-phase stator windings that present the peak back EMF are excited by properly switching the active switches of the inverter to produce a current with a quasi-rectangular shape. There are six combinations of the stator excitation over a fundamental cycle; each combination lasts for a phase period of π/3, as depicted in Fig. 1. The corresponding two active switches in each period may perform pulse width modulation (PWM) to regulate the motor current. To reduce current ripple, it is often useful to have one switch doing PWM while keeping the other conducting, instead of having the two switching simultaneously. It is also possible to split each of the six phase periods into segments and alternate the switch doing PWM during each segment to improve the current waveform or to prevent the unwanted circulating current that may occur in the inactive phase. It is assumed in the rest of this paper that only the upper three switches perform PWM, because this method is commonly used due to ease of implementation.

In order to provide such excitation currents, the rotor position information, i.e., the angular phase orientation of the back EMFs, must be known. Only the phase information at the six commutation instants per electrical cycle marked by arrows in the figure is required to control a BLDC motor.

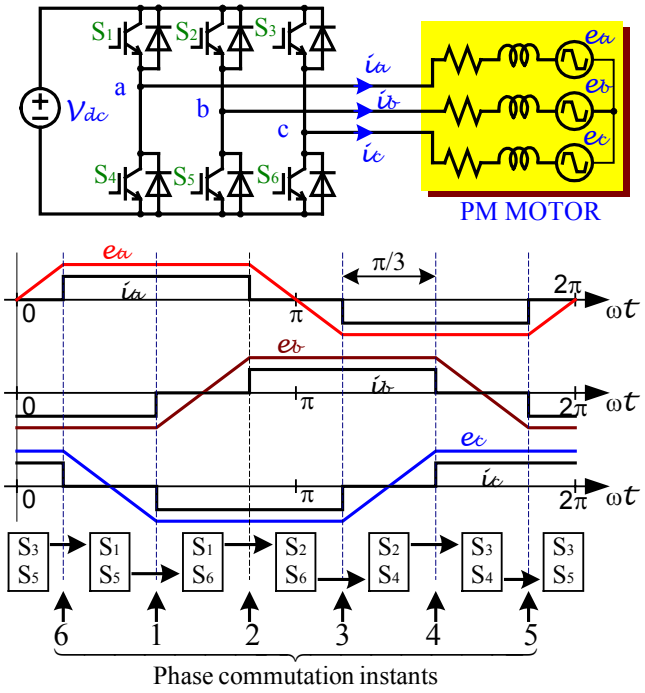

Fig. 1. Excitation of brushless dc motors.

B. Position Detection Based on Indirect Back EMF Sensing

As indicated in Fig. 1, only two of the three state-windings are excited at a time; and the third phase is open during the transition periods between the positive and negative flat segments of the back EMF. This arrangement provides a window to sense the back EMF, and this window rotates among the three phases as the stator current commutates from one phase to another. Therefore, each of the motor terminal voltages contains the back EMF information that can be used to derive the commutation instants. Fig. 2 shows simulated waveforms of terminal voltages, v_a, v_b and v_c, referred to the neutral point of a three-phase resistor network of wye connection attached to the motor terminals. The clean segments on the voltage waveforms correspond to the back EMFs.

Fig. 3 shows a traditional sensorless control scheme for a BLDC motor, where (a) shows a block diagram of the position detection circuit based on sensing all three motor-terminal voltages and (b) illustrates ideal operating waveforms for extracting the phase commutation timing information. Each of the motor terminal voltages, $v_{a'}$, $v_{b'}$ and $v_{c'}$, is fed into an integrator through a voltage divider of a resistor network. Ideally, the integrator in each phase introduces a phase shift of π/2 from the zero-crossings of the back EMFs. Detecting the zero-crossing instants of the integrator output generates the required phase-commutation timing signals.

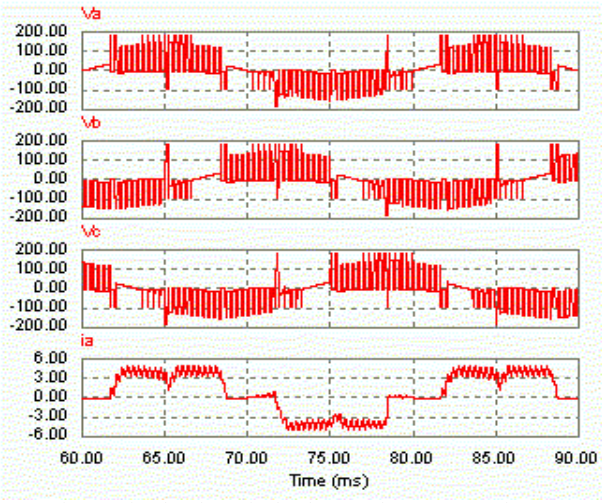

Fig. 2. Simulated terminal voltage and current waveforms.

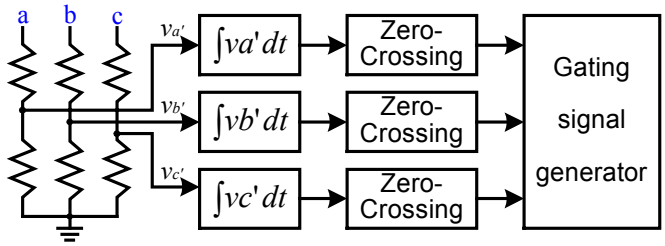

(a) Rotor position sensing circuit using all three motor-terminal-voltages

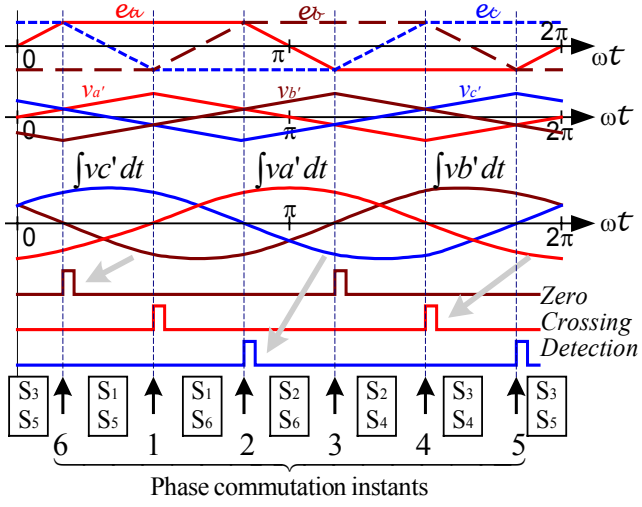

(b) Operating waveforms

Fig. 3. Traditional sensorless control scheme of BLDC motors.

The commutation signals can then be fed to a microprocessor through opto-couplers or pulse transformers for isolation. The microprocessor produces gate control signals for the inverter and may perform closed-loop speed control with the motor speed information measured by the frequency of the detected signals. Alternatively, inverter gating signal generator logic may be used if no closed-loop speed control is required.

The actual terminal voltages, $v_{a'}$, $v_{b'}$ and $v_{c'}$, contain chopped pulses generated by the switching operation of the inverter, as shown in Fig. 2. The use of an integrator not only filters out these voltage spikes, but also produces a signal of fixed amplitude that is dependent on the back EMF constant but independent of motor speed. This means, at least theoretically, that this scheme could work down to zero speed. In practice, however, one cannot use an integrator because of offsets and drifting that are inevitable in integrated circuits. Instead, low-pass filters are used to sense the terminal voltages, an arrangement which leads to a limited operating speed range for this scheme as the phase delay angle decreases with speed. This subject will be discussed in detail in the following section.

III. Proposed Low-Cost Sensorless Control Scheme for Brushless DC Motors

A. Simplified Position Detection Circuits

It is apparent from the previous section that sensing each terminal voltage can provide two commutation instants. Based on measuring the time between these two instants, it is possible to interpolate the other four commutation instants, assuming motor speed does not change significantly over consecutive electrical cycles. The circuit for sensing the other two terminal voltages can therefore be eliminated, leading to a 66% reduction in sensing components.

Fig. 4 illustrates the proposed low-cost sensorless control scheme for BLDC motors, where (a) shows a block diagram of the position detection circuit based on sensing only one motor-terminal voltage and (b) illustrates ideal operating waveforms for extracting the phase commutation timing information. Phase voltage, $v_{a'}$, is fed into an integrator for filtering and introducing the necessary phase delay. Detecting the zero crossing of the integrator output, $v_{a''}$, produces two commutation instants per fundamental cycle. This information is then fed into a microprocessor. The microprocessor measures the elapsed time, T_k, between these two instants and generates the other two commutation instants apart from the last sensed instant by $T_k/3$ and $2T_k/3$, respectively. Because of the use of interpolation, this scheme works best for applications that do not require frequent, rapid acceleration or deceleration, usually encountered in BLDC motor applications.

B. Correction of Position Detection Errors

As mentioned before, an ideal integrator cannot be used in practice. Instead, a low-pass filter is employed to extract the phase information from the back EMF as shown in Fig. 5(a). The phase delay introduced by the filter varies with the back EMF frequency, i.e., the motor speed, and is always less than $\pi/2$. This speed-dependent phase-delay characteristic, if not corrected, will produce incorrect phase-commutation timing. The graph shown in Fig. 5(b) plots the phase delay versus frequency for a typical filter design. The phase shift is close to the required 90 degrees at the rated frequency of 50 Hz but drops as the frequency is reduced.

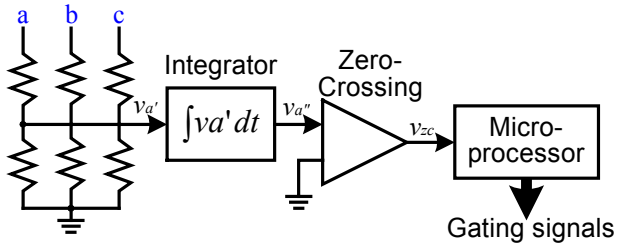

(a) Rotor position sensing circuit using only one motor-terminal voltage

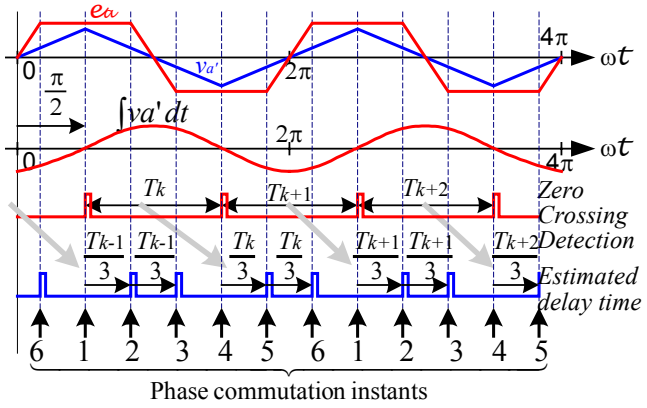

(b) Phase voltages and currents for a BLDC

Fig. 4. Proposed low-cost sensorless control scheme for BLDC motors.

Fig. 5(c) shows simulated current waveforms at 20 Hz with a phase delay less than 90 degrees. The insufficient phase delay of the filter causes three major problems at low speed. The first is a decrease in the torque-per-ampere capability because stator currents are not provided throughout the entire time that the phase back EMFs are at peak level. This leads to the second problem, torque ripple. The third is the additional copper loss produced by a circulating current flowing in the supposedly opened phase. This circulating current results from the shorting of the corresponding two phase-back-EMFs through the switch that is turned on and the diode associated with the switch that is turned off in the process of phase commutation between the lower switches. Take for instance the commutation from phase-*c* to phase-*a* and refer to Fig. 1. At the beginning of each negative half-cycle of i_a when the motor current is commutated by switching off S_6 and switching on S_4 while S_2 is conducting, the diode of S_6 is positively biased because back EMF, e_a, is greater than e_c. Therefore, the two back EMFs are shorted through the diode and S_4, and consequently a circulating current is produced. Notice that commutations between the upper switches will not produce a circulating current because of the PWM switching operation.

To satisfactorily operate a motor at low speeds, the phase errors need be corrected. Once the filter is designed, the resulting phase delay at a given frequency can be calculated. This can be done online or offline to construct a look-up table. Fig. 5(d) shows operating waveforms with phase-error correction. The correction is based on measuring the elapsed time, T_k, between the last two zero-crossing instants and converting it to frequency according to $fm=1/(2T_k)$. With this frequency information, the delay time correction, τ_k, can then be determined.

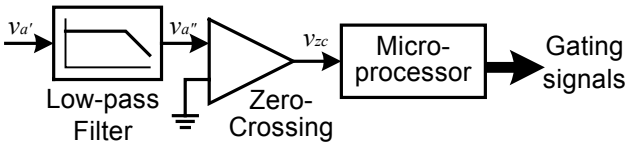

(a) Rotor position sensing circuit using a low-pass filter

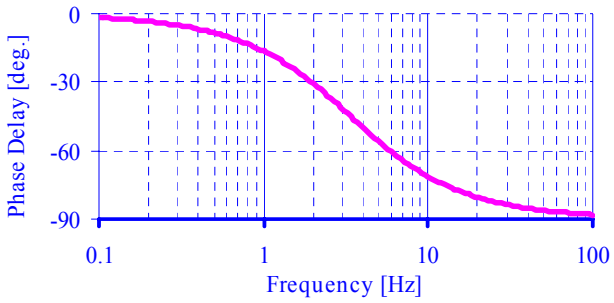

(b) Phase delay vs. frequency for a typical low-pass filter design

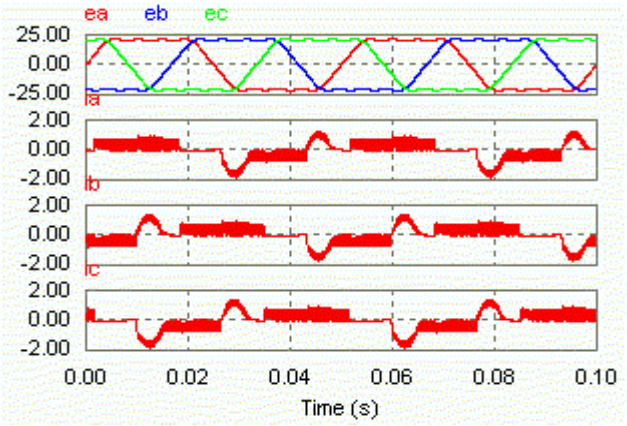

(c) Simulated waveforms showing circulating current with a phase-delay < π/2

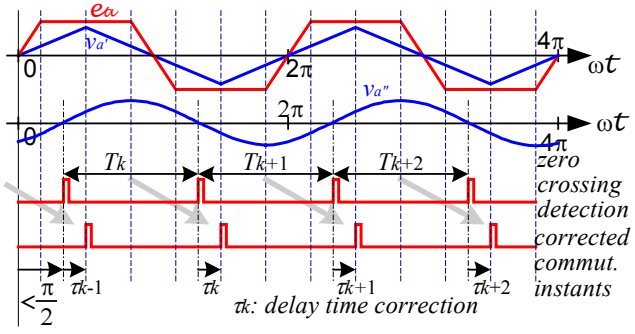

(d) Operating waveforms showing delay time correction

Fig. 5. Position sensing scheme using a low-pass filter with phase-delay correction.

Fig. 6 shows an alternative sensing scheme, based on a band-pass filter, to further eliminate two branches of the resistor network. The terminal voltage referred to the negative

dc bus rail, $v_{a'}$, is fed into the band-pass filter to remove the dc component and high-frequency content resulting from the PWM operation. The filtered voltage, $v_{a''}$, is then passed to a comparator to detect the zero-crossing instants, which are further sent to a microprocessor for phase-delay correction and generation of commutation signals in a way similar to that described in the previous section.

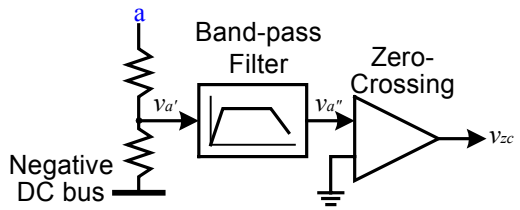

Fig. 6. An alternative sensing scheme.

C. Microprocessor Based Implementation of Sensorless Control

Fig. 7 shows a microprocessor-based implementation of the suggested position detection scheme for speed control. The zero-crossing signals from the detection block [Fig. 5(a) or Fig. 6], v_{zc}, are fed to the microprocessor through an interrupt input, which activates an interrupt service routine (ISR) to read a timer, Tm_1, and to calculate the time, T_k, between the last two interrupts. This measured time is converted to frequency according to $fm=1/(2T_k)$, which is in turn used as an index to a time-delay correction table. The time-delay correction, τ_k, is loaded into the counter of a second timer, Tm_2, which starts counting down to zero. Upon reaching zero, it generates an interrupt to a second ISR, which generates a phase commutation signal and starts a third timer, Tm_3, whose counter was loaded with $T_k/3$. Tm_3 counts down to zero and generates an interrupt to a third ISR, which generates a phase commutation signal, reloads Tm_3 with $T_k/3$, and starts counting again. Upon the second interrupt, the third ISR generates a phase commutation signal and stops Tm_3.

A proportional-integral (PI) controller is used for speed regulation. A feed-forward path with a gain equal to the back EMF constant, K_{bemf}, is also added to improve the speed control response. Speed feedback is furnished by the first ISR, which has a resolution of $2\times P$ pulses per revolution, where P is the pole pair number of the motor. For simplicity, no current control loop is provided. A fourth timer, Tm_4, is used to generate a PWM duty control signal, which is gated to one of the upper switches, S_1, S_2 or S_3, by the commutation signals from the timer, Tm_3. It is assumed that only the upper three devices of the inverter are performing PWM to regulate the current of the motor, and the lower switches conduct for a fixed period of 120 electrical degrees corresponding to the negative flat portion of each phase back EMF in each cycle.

A starting control block manages the timers, Tm_3 and Tm_4, for an initial startup of the motor when no position information is available. It performs rotor alignment and then provides the motor with a current whose frequency is increased in a linear manner from a low starting value. The motor is forced to rotate synchronously with the currents. Once the motor reaches the speed at which the back EMF can be reliably detected, the speed regulation loop takes control and the motor continues to accelerate to a desired speed.

IV. Experimental Results

Fig. 8 shows a laboratory implementation of the suggested position detection scheme for speed control of a PM motor. A standard bridge inverter with a six-pack transistor module is used to provide necessary current control for the motor. Only the upper three transistors are performing PWM to regulate the current of the motor. The PWM carrier frequency was set at 3 kHz. Ratings and parameters of the PM motor are listed as: power = 2.2 kW; torque = 14 Nm; current = 12.5 Arms; resistance = 0.26 Ohm; inductance = 5 mH; number of poles = 4; speed = 1500 rpm.

As shown in Fig. 8, the voltage across terminal c and the negative dc bus rail, v_{cn}, is used for position sensing. A band-pass filter was employed with a phase-delay characteristic given in Fig. 9. At a given frequency, the phase delay of this band-pass filter is smaller than that of the low-pass filter shown in Fig. 5(b). Moreover, it changes from phase delay to phase leading as the frequency drops below 2.5 Hz.

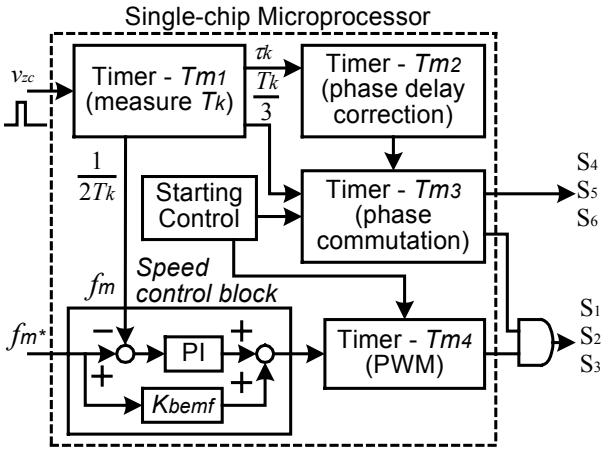

Fig. 7. Microprocessor implementation of the proposed sensorless control.

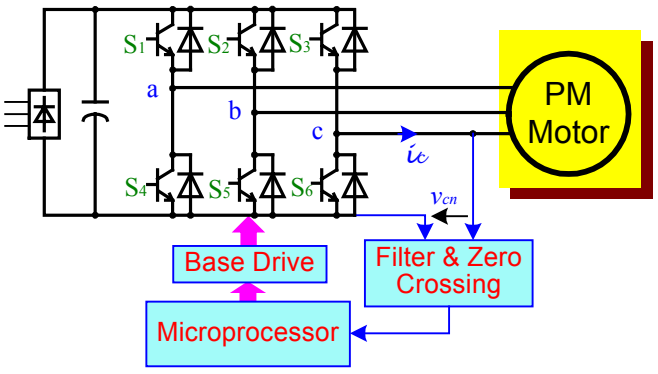

Fig. 8. Lab implementation of position and speed sensor-less control.

Fig. 10 gives typical oscillograms of no-load current, i_c, and voltage, v_{cn}, waveforms at 390, 750 and 1500 rpm. Fig. 10 (a) was recorded without the correction of position error resulting from the back EMF detection filter. For comparison, Fig. 10 (b) shows the corresponding waveforms when the position error is corrected. Without the correction, a circulating current flows at the beginning of each half-cycle because the currents are phase-leading the back EMFs. Fig. 10 (c) and (d) show the waveforms at higher speed illustrating proper phase delay correction and no circulating current.

Fig. 11 shows typical current and voltage waveforms when the motor was loaded with a rated torque at 750 rpm, indicating no circulating current.

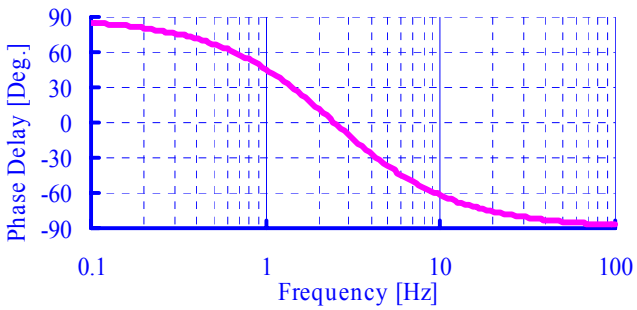

Fig. 9. Phase shift introduced by the band-pass filter.

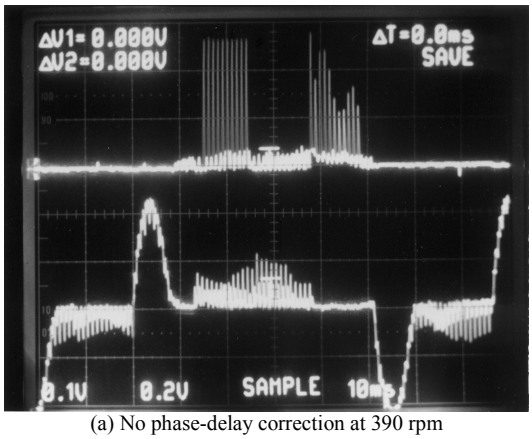

(a) No phase-delay correction at 390 rpm

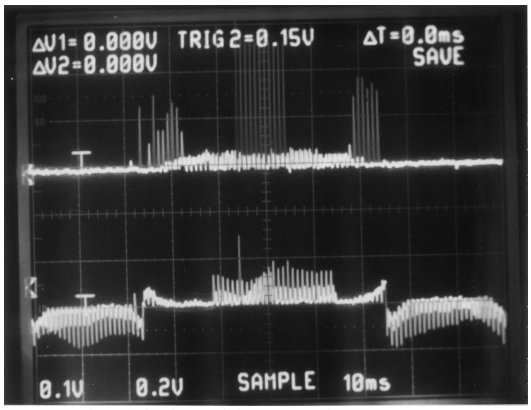

(b) With phase-delay correction at 390 rpm

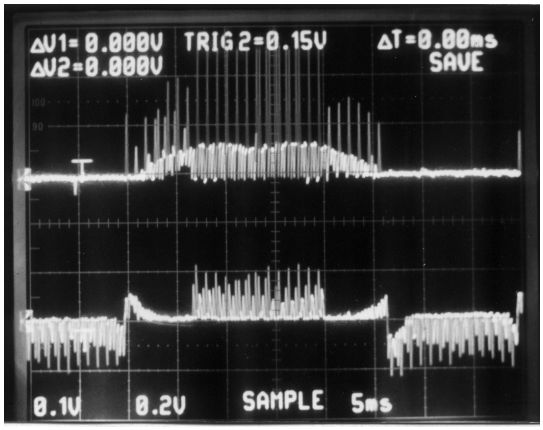

(c) With phase-delay correction at 750 rpm

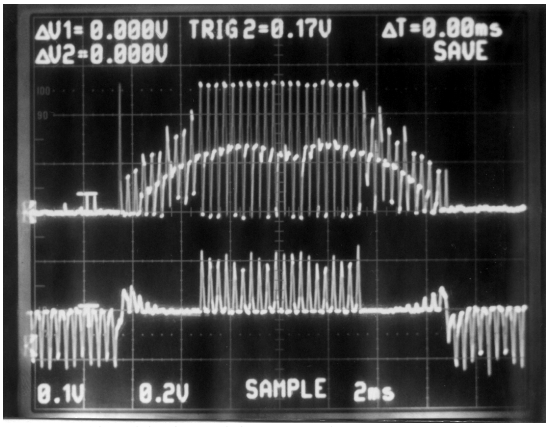

(d) With phase-delay correction at 1500 rpm

Fig. 10.Experimental voltage and current waveforms. Top: v_{cn}, 110V/div, Bottom: i_c, 1A/div.

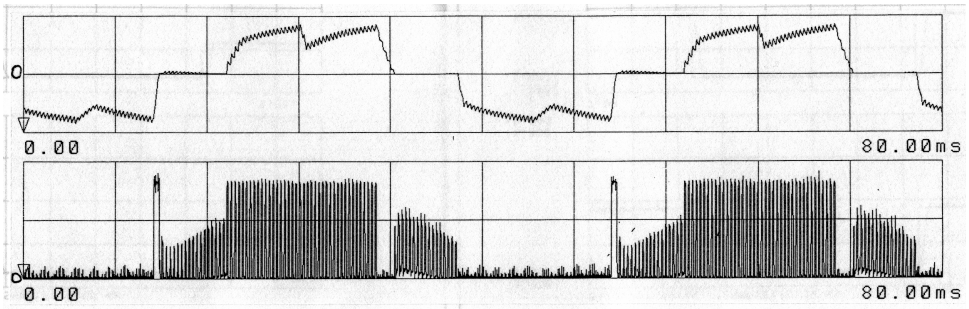

i_c, 30A/div

v_{cn}, 170V/div

Fig. 11. Experimental voltage and current waveforms when loaded with a rated torque load at 750 rpm.

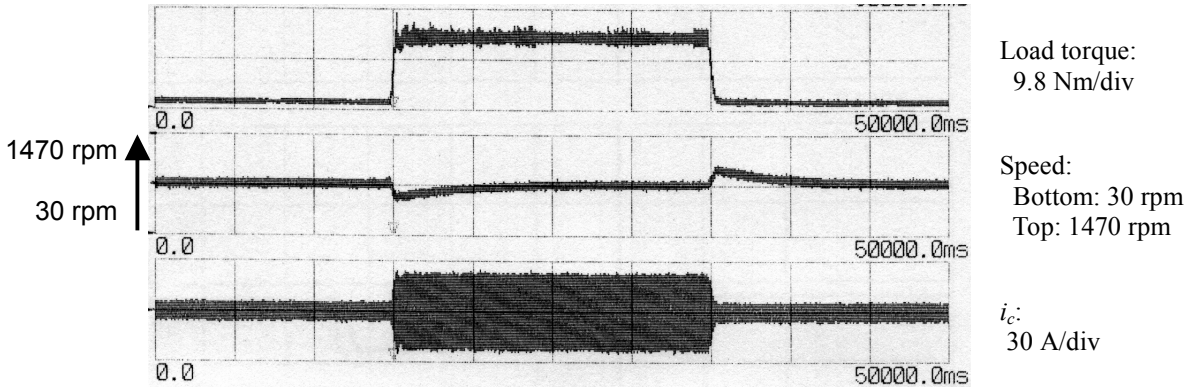

Fig. 12.Dynamic response to step changes in load torque by switching on and off a rated load torque while the motor is commanded at a speed of 750 rpm.

Fig. 12 shows a dynamic response of motor speed to step changes in load torque caused by switching on and off a rated load torque when the motor was commanded at a speed of 750 rpm, indicating stable speed control.

Fig. 13 compares the PM motor efficiency as a function of speed with a constant rated torque load for the proposed and the conventional sensing scheme without phase-delay compensation. Around the rated speed of 1500 rpm, both sensing methods offer a very close efficiency. As the motor speed decreases, so does the efficiency, because the motor was designed for maximum efficiency at rated load and rated speed. However, the efficiency drops faster with the conventional sensing scheme because the phase delay introduced by the low-pass filters decreases with the motor speed. This incorrect phase delay makes the motor inoperable as the speed reaches 300 rpm. The operating range is from 100 to 1500 rpm for the proposed sensing scheme with phase-delay correction.

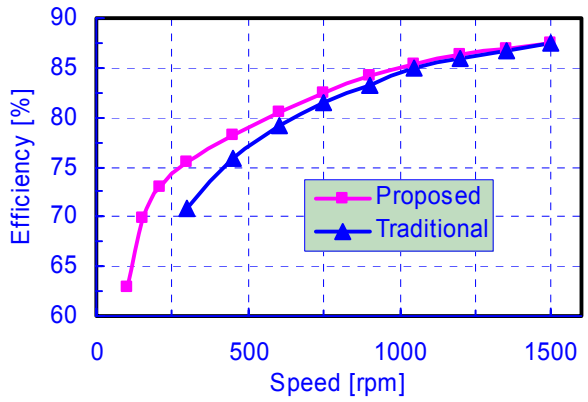

Fig. 13.Comparison of measured efficiency vs. speed at a full load torque.

V. Conclusions

This paper presents a low-cost position and speed sensorless control scheme for brushless dc motors. Cost saving is achieved by significantly reducing the number of components in the position sensing circuit and by coupling the sensing circuit with a single-chip microprocessor for speed control.

In addition, the filter phase-delay correction method can

- extend control into significantly lower speeds by eliminating the position detection errors, which are significant at low speeds, and
- reduce torque ripple and improve motor efficiency by always maintaining the motor currents in phase with the back EMFs.

The proposed scheme has been successfully verified by analytical and experimental results.

References

[1] D. M. Erdman, H. B. Harms, J. L. Oldenkamp, "Electronically Commutated dc Motors for the Appliance Industry," *Conf. Rec. 1984 IEEE Ind. Applicat. Soc. Ann. Mtg.*, pp. 1339-1345.

[2] T. Endo, F. Tajima, H. Okuda, K. Iizuka, Y. Kawaguchi, H. Uzuhashi, Y. Okada, "Microcomputer-Controlled Brushless Motor without a Shaft-Mounted Position Sensor," *IPEC-Tokyo'83 Conf. Record*, pp. 1477-1488, March 1983.

[3] K. Iizuka, H. Uzuhashi, M. Kano, T. Endo, and K. Morhri, "Microprocessor Control for Sensorless Motor," *IEEE Trans. Ind. Applicat.* Vol. IA-21, pp. 595-601, Aug. 1985.

[4] S. Ogasawara and H. Akagi, "An Approach to Position Sensorless Drive for BLDCM," *IEEE Trans. Ind. Applicat.*, vol. IA-27, no. 5, pp. 928-933, Sept./Oct. 1991.

[5] R. Wu and G. R. Slemon, "A Permanent Magnet Motor Drive without a Shaft Sensor," *IEEE Trans. Ind. Applicat.*, vol. IA-27, no. 5, pp. 1005-1011, Sept./Oct. 1991.

[6] I. Takahashi, T. Koganezawa, G.-J. Su, K. Ohyama, "A Super High Speed PM Motor Drive System by a Quasi-Current Source Inverter," *IEEE trans. Ind. Applicat.*, vol. 30, pp. 683-690, May/June 1994.

[7] J. C. Moreira, "Indirect Sensing for Rotor Flux Position of Permanent Magnet AC Motors Operating Over a Wide Speed Range," *IEEE Trans. Ind. Applicat.* Vol. IA-32, pp. 1394-1401, Nov./Dec. 1996.

[8] D.-H. Jung and I.-J. Ha, "Low-Cost Sensorless Control of Brushless dc Motors Using a Frequency-Independent Phase Shifter," *IEEE Trans. Power Electron.*, vol. PELS-15, pp. 744-752, Jul. 2000.

[9] G.-J. Su, G. W. Ott, J. W. McKeever, K. S. Samons, R. L. Kessinger, "Development of a Sensor-less Speed Control Inverter for an Automotive Accessory Permanent Magnet Motor", *CD-ROM Proc. Of 2001 Future Car Congress*, Arlington, Va., April 2001.

[10] T. M. Jahns, "Torque Production in Permanent-Magnet Synchronous Motor Drives with Rectangular Current Excitation," *IEEE Trans. Ind. Applicat.*, vol. IA-20, pp. 803-813, Jul./Aug. 1984.